The Astrophysical Journal, 685: L141–L144, 2008 October 1


# TURBULENT ENTRAINMENT IN MIRA'S COMETARY TAIL

A. C. Raga[1] and J. Cantó[2]
*Received 2008 June 11; accepted 2008 August 14; published 2008 August 28*


## ABSTRACT

Mira is a red giant star which passes through the Galactic ISM, leaving behind a cometary tail extending over ∼2° (seen in the spectacular UV image of Martin and coworkers). H I 21 cm emission from this cometary tail has now also been detected. The 21 cm emission shows a velocity that decreases monotonically with increasing distances from Mira (along the axis of the cometary tail). We present a "turbulent wake" model which gives a simple, analytic prediction for the velocity of the material in the wake as a function of distance from the stellar wind source. We fit this predicted velocity versus position law to the velocities deduced from the 21 cm observations, and find that a wake with a half-opening angle of ≈11.8° (and a stellar motion and wind velocity/mass-loss rate corresponding to the values determined for Mira) reproduces the observations.


*Subject headings:* circumstellar matter — hydrodynamics — ISM: jets and outflows — stars: AGB and post-AGB — stars: individual (Mira)

## 1. INTRODUCTION

Martin et al. (2007) discovered a remarkable cometary structure which trails the passage of Mira through the ISM in the Galactic plane. The emission of the tail of Mira's comet extends over ≈2° in a UV map with central wavelength $\lambda_c = 1516$ Å and a FWHM $\Delta\lambda = 256$ Å. This emission might come from fluorescent $H_2$ lines (see Martin et al. 2007).

The cometary structure was modeled numerically by Wareing et al. (2007) as the interaction of a stellar wind from a red giant star moving at a high spatial velocity with respect to the surrounding ISM. Raga et al. (2008) computed a similar model, but introducing an anisotropy in the wind ejection (consistent with the fact that Mira's wind is observed to have strong deviations from axisymmetry; see Josselin et al. 2000).

The recent observations of the H I 21 cm emission of Mira's comet (Matthews et al. 2008) represent a large step forward in providing information for constraining models of this object. These authors present interferometric maps in which they detect 21 cm emission in a region of ∼5′ around Mira. They also present single-dish observations in which they detect the 21 cm line out to ∼2° along Mira's tail, showing a radial velocity which decreases from ≈45 km s$^{-1}$ (at the position of Mira) to ≈28 km s$^{-1}$ (at a distance of ≈1.5°).

In the present Letter, we propose a "turbulent wake" model in order to interpret this decreasing velocity versus position law. This model is based on mass and momentum conservation considerations, following the approach for modeling turbulent jets of Bicknell (1984) and for turbulent mixing layers of Cantó & Raga (1991).

The Letter is organized as follows. In § 2 we summarize the observational results of the Mira system that are relevant in the context of our model. In § 3 we present the analytic model, derive the theoretical velocity versus position law (along the cometary tail), and carry out a least-squares fit to the velocity law obtained from the 21 cm observations of Matthews et al. (2008). In § 4 we use the model parameters in order to derive the physical parameters required for the star (i.e., the motion of the star and the properties of its wind), and compare them with the observationally determined parameters. The approximations of the model are discussed in § 5. Finally, we present our conclusions in § 6.

## 2. OBSERVATIONS

In this section, we summarize the relevant observations of Mira and its cometary structure which are relevant for our application to this object of a turbulent wake model.

From observations with the *Hipparcos* satellite, a distance $D = 107$ pc (Knapp et al. 2003) and a proper motion of 115 km s$^{-1}$ (Turon et al. 1993) have been determined. For the radial velocity of Mira, we adopt the value of 46.7 km s$^{-1}$ determined from CO observations by Winters et al. (2003). We note that this radial velocity differs quite substantially from the older value of Evans (1967). From these velocities, we calculate a spatial velocity $v_* = 124.1$ km s$^{-1}$ and an orientation angle $\phi = 22°$ (between the motion of Mira and the plane of the sky).

Matthews et al. (2008) have obtained interferometric and single-dish H I 21 cm observations of Mira's comet. From their single-dish data, they have obtained measurements of radial velocity as a function of position along the tail of the cometary structure. With the $\phi = 22°$ orientation angle derived above and the $D = 107$ pc distance to Mira, we have corrected the radial velocities and the positions in order to obtain the velocity along the tail as a function of the distance from Mira. In order to correct the velocities, we have assumed that the observed radial velocities correspond to the projection along the line of sight of a flow velocity oriented along the axis of the cometary tail. The result of this exercise is shown in Figure 1.

From the UV maps of Martin et al. (2007), we can estimate the size of the head. We estimate two sizes: the bow shock standoff distance $d_s \approx 3' \approx 3 \times 10^{17}$ cm (see Wareing et al. 2007) and the width of the tail measured across the position of Mira $2r_0 \approx 8' \approx 7.7 \times 10^{17}$ cm. The definitions of $d_s$ and $r_0$ are shown in the schematic diagram of Figure 2 (see § 3).

Finally, Ryde et al. (2000) have analyzed observations and models for Mira's wind. From their analysis, they propose different possible configurations, and Martin et al. (2007) have taken an average of the proposed values, obtaining a $v_w = 5$ km s$^{-1}$ wind velocity and a $\dot{M}_w = 3 \times 10^{-7}\ M_\odot$ yr$^{-1}$ mass-loss rate.

[1] Instituto de Ciencias Nucleares, Universidad Nacional Autónoma de México, Apartado 70-543, 04510 D.F., México; raga@nucleares.unam.mx.
[2] Instituto de Astronomía, Universidad Nacional Autónoma de México, Apartado 70-264, 04510 D.F., México.

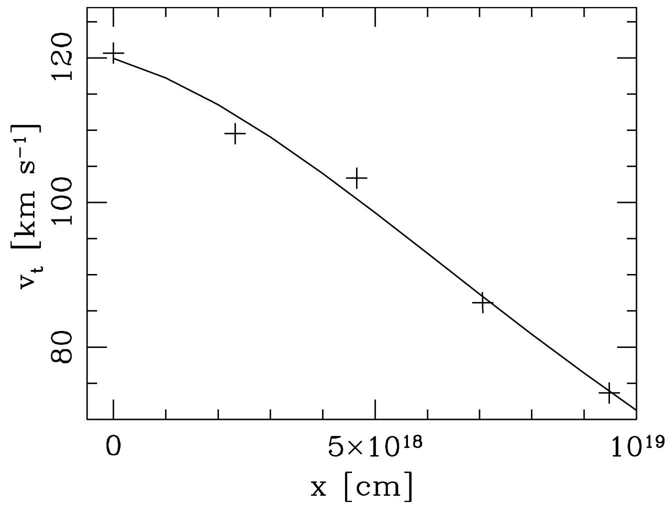


FIG. 1.—Velocity $v_t$ along the cometary tail as a function of distance $x$ from Mira, deduced by deprojecting the 21 cm radial velocity measurements of Matthews et al. (2008). The velocities deduced from the observations are shown with the crosses, and the continuous curve shows the fit to the data of our turbulent wake model (see eq. [4]).

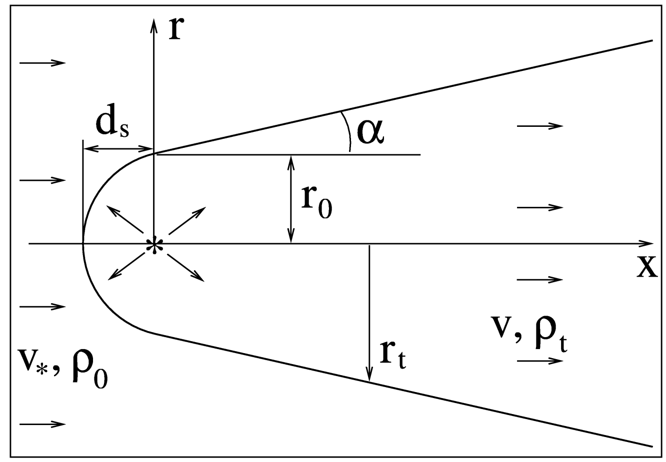


FIG. 2.—Schematic diagram showing the interaction of a stellar wind with a streaming environment. In a reference system at rest with the star, the environment (with a homogeneous density $\rho_0$) flows at a velocity $v_*$ along the $x$-axis. The star is at the origin of the coordinate system. The stellar wind bow shock has an on-axis standoff distance $d_s$. For $x > 0$, the bow shock wings are assumed to be conical, with a half-opening angle $\alpha$. The flow along the tail is assumed to be well mixed, and has an average density $\rho_t$ and an average velocity $v$ (along the symmetry axis).

## 3. THE TURBULENT WAKE

We model Mira's cometary tail as a turbulent wake. In Figure 2 we show the configuration of the flow in a reference system moving with Mira, so that the surrounding interstellar medium (assumed to have a homogeneous density $\rho_0$) streams by with a velocity $v_*$. This flow interacts with the wind from Mira (with a mass-loss rate $\dot{M}_w$ and a terminal velocity $v_w$), forming a bow shock. The star is located at the origin of the ($x$, $r$) cylindrical coordinate system (see Fig. 2), and the ISM flows in the $+x$-direction. We assume that the wind is stationary and isotropic.

At $x = 0$, the cylindrical radius of the bow shock has a value $r_0$, which is fixed by the observed width of Mira's comet (see § 2). This is the initial cylindrical radius of the "turbulent wake" present in the $x > 0$ region of the flow.

We now derive a model for the turbulent wake region of the flow (i.e., the $x > 0$ region; see Fig. 2). We first assume that the tail has a constant opening angle $\alpha$, so that the cylindrical radius $r_t$ of the tail is given by

$$r_t = r_0 + x \tan \alpha. \tag{1}$$

We now consider the mass conservation equation

$$\pi r_t^2 \rho_t v = \dot{M}_w + \pi r_t^2 \rho_0 v_* \tag{2}$$

and the momentum conservation equation

$$\pi r_t^2 \rho_t v^2 = \pi r_t^2 \rho_0 v_*^2. \tag{3}$$

In equation (2), the term on the left-hand side represents the mass going through a cross section of the wake (at position $x$ along the symmetry axis; see Fig. 2). In this term, $v$ is an average of the axial velocity and $\rho_t$ an average of the density over the cross section of the wake. The right-hand term of equation (2) is the addition of the mass $\dot{M}_w$ injected (per unit time) by the star, and the environmental mass rate $\pi r_t^2 \rho_0 v_*$ intercepted by the bow shock + tail structure. In equation (3) the term on the left represents the momentum rate going through a cross section of the wake (at position $x$), and the right-hand side term is the momentum rate of the environmental material intercepted by the bow shock + tail structure (the isotropic stellar wind has zero net momentum).

In equations (2)–(3) there is an implicit assumption of efficient mixing of the material within the wake. The gas which is entrained through the oblique edges of the bow shock (at $r > r_0$; see Fig. 2) has to be efficiently incorporated into the rest of the "tail flow," initially composed of the stellar wind and ISM material which went through the head of the bow shock. The well-mixed flow within the tail has radial density and velocity profiles, and $\rho_t$ and $v$ are average values calculated with these radial profiles.

Equations (1)–(3) can be combined to obtain

$$v_t \equiv v_* - v = \frac{v_*}{1 + (a + x/d)^2}, \tag{4}$$

where

$$a \equiv \frac{r_0}{d_0}, \quad d \equiv \frac{d_0}{\tan \alpha}, \quad d_0 \equiv \sqrt{\frac{\dot{M}_w}{\pi \rho_0 v_*}}. \tag{5}$$

In equation (4), $v_t$ is the velocity of the wake material (averaged over the cross section of the tail) measured in a reference frame at rest with respect to the ambient medium, so that it can in principle be compared directly with the observed velocity versus position law (see § 2).

We now carry out a least-squares fit of equation (4) to the tail velocities (see Fig. 1) deduced from the H I observations of Matthews et al. (2008). From the fit of equation (4) to the measured velocities, we obtain

$$a = 0.13, \quad d = 1.40 \times 10^{19}\,\mathrm{cm}, \quad v_* = 122\ \mathrm{km\ s^{-1}}. \tag{6}$$

While the errors in the parameters deduced from the fit are small (of ∼10%), one should be aware that the rather extreme simplifications of the model imply that the physical parameters that we will deduce below should only be considered as rough estimates.

## 4. THE PHYSICAL PARAMETERS DEDUCED FROM THE TAIL MODEL

We now consider that the initial cylindrical radius of the tail is $r_0 \approx 3.8 \times 10^{17}$ cm (see § 2). From equations (5) and (6) we then obtain $d_0 = 2.9 \times 10^{18}$ cm and $\alpha = 11.8°$. From the fit, we also obtain a $v_* = 122$ km s$^{-1}$ value for the motion of the star with respect to the surrounding medium (see eq. [6]), which compares very well with the 124 km s$^{-1}$ spatial motion of Mira (see § 2).

We can also use the fact that the on-axis standoff distance $d_s$ (see Fig. 2) of Mira's bow shock has a value $d_s = 3.1 \times 10^{17}$ cm (see § 2). From the usual wind/ambient medium ram pressure balance condition, $d_s$ is given by

$$d_s = \sqrt{\frac{\dot{M}_w v_w}{4\pi \rho_0 v_*^2}}, \tag{7}$$

where $v_w$ is the terminal velocity of the isotropic wind. From equations (5) and (7) we obtain

$$\frac{v_w}{v_*} = 4\left(\frac{d_s}{d_0}\right)^2 = 0.046, \tag{8}$$

where the numerical value was obtained setting $d_s = 3.1 \times 10^{17}$ cm and $d_0 = 2.9 \times 10^{18}$ cm (see above). We then obtain a wind velocity $v_w \approx 5.7$ km s$^{-1}$ (using a $v_* = 124$ km s$^{-1}$ stellar motion velocity). This value for $v_w$ also agrees very well with an ≈5 km s$^{-1}$ average wind velocity of the values quoted by Ryde et al. (2000) for Mira (also see § 2).

Furthermore, we can estimate the density $\rho_0$ of the surrounding ISM by using the definition of $d_0$ (see eq. [5]), the $d_0 = 2.9 \times 10^{18}$ cm determined from the fit to the observed tail velocity versus position and the $\dot{M}_w = 3 \times 10^{-7}\, M_\odot$ yr$^{-1}$ mass-loss rate of Mira (see § 2). We obtain $n_0 = \rho_0/(1.3 m_{\rm H}) = 0.03$ cm$^{-3}$ (where $m_{\rm H}$ is the H mass). This value coincides with the ISM density derived by Wareing et al. (2007) from the observed value of the standoff distance $d_s$ of Mira's bow shock and the ram pressure balance relation (eq. [7]).

## 5. THE VALIDITY OF THE MODEL ASSUMPTIONS

The three main assumptions in the analytic model are that the flow is stationary, that it is well mixed, and that the tail is conical.

The assumption of a steady flow is of course somewhat unintuitive for modeling a turbulent flow, which in principle has a complex structure of time-dependent turbulent eddies. When considering a steady flow, one is attempting to describe a statistically steady, average "mean flow" on which are superimposed the time-dependent, turbulent eddies.

The assumption of a well-mixed flow can be evaluated by considering the linear growth rate of a Kelvin-Helmholtz mode of wavelength $\sim r_0$:

$$\tau_{\rm KH} = \frac{r_0}{v}\,\frac{(\rho_1 + \rho_2)}{2\pi\sqrt{\rho_1 \rho_2}}, \tag{9}$$

where $r_0$ is the initial radius of the tail (see Fig. 2), $\rho_1$ and $\rho_2$ are the densities on the two sides of the shocked ISM/stellar wind boundary, and $v$ is the relative velocity between the two media. Noting that the density-dependent term in equation (9) is of order unity (because the $\rho_1/\rho_2$ density ratio is of the order of $(T_2/T_1)^{1/2} \sim 10$, where $T_1$ and $T_2$ are the temperatures on both sides of the boundary) and that $v \sim v_*$, we conclude that $\tau_{\rm KH} \sim r_0/v_*$. In this timescale, the perturbation will have traveled a distance $x_{\rm KH} \sim r_0$ along the tail axis.

From this discussion, one would conclude that the tail will be fully turbulent for distances $x > r_0$ along the cometary tail. For this region, the assumption of a well-mixed flow should be approximately correct. We also note that this result is consistent with the results from the numerical simulations of Wareing et al. (2007) and Raga et al. (2008), in which the tail flow develops turbulence relatively close to the star.

The assumption of a constant opening angle for the tail is consistent with the numerical simulations of Pittard et al. (2005). The simulations of Wareing et al. (2007) and Raga et al. (2008) produce tails which have a general trend of growing widths as a function of distance from the star, but show complex, large eddy structures. This difference arises from the fact that in the work of Pittard et al. (2005) a parameterized "turbulent dissipation" was included, so as to obtain a simulation of the "mean flow" (averaged over the short-lived turbulent eddies), more in line with our present work, which also attempts to obtain a description of the mean flow.

## 6. CONCLUSIONS

Matthews et al. (2008) have mapped the H I 21 cm emission of the tail of Mira's comet. They detect a substantial decrease in radial velocity (from ≈45 down to 28 km s$^{-1}$) over ≈91′. When corrected for the $\phi \approx 22°$ orientation (between the motion of Mira and the plane of the sky), and at a distance of 107 pc, the observations result in the velocity versus position relation shown in Figure 1, with a drop from ≈120 km s$^{-1}$ at the position of Mira down to ≈75 km s$^{-1}$ at a distance of ≈$10^{19}$ cm along the cometary tail.

We present a simple, turbulent wake model. In this model, we assume that the stellar wind and the ISM intercepted by the stellar wind bow shock mix together in order to produce a turbulent wake flow. Furthermore, we assume that the tail (bounded by the extended wings of the bow shock) is conical.

From this model, we obtain the axial velocity $v_t$ as a function of position $x$ along the tail (see eq. [4]). The free parameters of the model are the stellar velocity $v_*$, $a = r_0/d_0$, and $d = d_0/\tan\alpha$, where $r_0$ is the initial radius and $\alpha$ is the half-opening angle of the tail ($d_0$ is defined in eq. [5]; also see Fig. 2). Through a least-squares fit to the deprojected velocity versus position observations (see Fig. 1), and the observed $r_0 = 3.8 \times 10^{17}$ cm initial tail radius, we obtain an opening angle $\alpha = 11.8°$ and a characteristic length $d_0 = 1.4 \times 10^{19}$ cm of the velocity decrease along the cometary tail (see eq. [4]). We also obtain $v_* = 122$ km s$^{-1}$, which is in excellent agreement with the velocity determined from radial velocity and proper motion observations of Mira (see § 2).

Now, using the observationally determined bow shock standoff distance $d_s = 3.1 \times 10^{17}$ cm (see § 2), the ram-pressure balance condition (eq. [7]), and the value of $d_0$ obtained from the fit to the velocities along Mira's tail (eq. [5]), we can compute the value of the wind velocity $v_w = 4 v_* (d_s/d_0)^2 = 5.7$ km s$^{-1}$ (see eq. [8]). This value lies well within the range of velocities proposed for Mira's wind in Ryde et al. (2000).

Another way of seeing this result is as follows. If we adopt the $v_w = 5$ km s$^{-1}$ wind velocity suggested by Martin et al. (2007; who took an average of the values given by Ryde et al. 2000), we can use the ram-pressure balance relation (eq. [7]) and the measured bow shock standoff distance to obtain the value of the $\dot{M}_w/\rho_0$ ratio. We can then use the $v_* = 124$ km $s^{-1}$ measured motion of Mira in order to fix the value of $d_0$ and $v_*$ in equations (4)–(5). Equation (4) then has a single free parameter, which is the opening angle $\alpha$ of the tail. A single-parameter least-squares fit to the observed velocity versus position dependence along the tail (see Fig. 1) would then give us the same $\alpha = 11.8°$ opening angle that we have determined from our three-parameter fit.

An interesting point is that our model predicts the formation of a broad tail, with a full opening angle $2\alpha \approx 24°$. This tail would look like the broad tails obtained from numerical simulations of isotropic wind/streaming environment interactions (see, e.g., Pittard et al. 2005; Wareing et al. 2007). These broad tails differ qualitatively from the narrower, very well collimated structure seen in the UV observations of Mira (Martin et al. 2007). In order to reconcile these results, one has to argue that the UV tail corresponds to an inner core of the turbulent tail structure left behind by Mira. This inner core could have a high enough shielding from external UV photons, allowing the survival of molecules such as $H_2$, which possibly produce the observed UV emission (see Martin et al. 2007).

We end by noting that our results represent an unprecedented success in comparing parameterized turbulent jet/wake models with astrophysical flows. Our effort is a first attempt to use the observations of Mira's comet to constrain a simple, parameterized turbulence model (in our model, the turbulence parameterization is implicitly included as a free opening angle for the wake). Clearly, more complex models of turbulent flows could be tested against the velocity versus position law obtained from the 21 cm observations of Mira's cometary tail. As new, more precise observations of this remarkable flow become available, this object will become a unique testing ground for models of hypersonic turbulence in astrophysical, radiative flows.

This work was supported by the CONACyT grants 46828-F and 61547, the DGAPA (UNAM) grant IN 108207, and the "Macroproyecto de Tecnologías para la Universidad de la Información y la Computación" (Secretaría de Desarrollo Institucional de la UNAM, Programa Transdisciplinario en Investigación y Desarrollo para Facultades y Escuelas, Unidad de Apoyo a la Investigación en Facultades y Escuelas). We thank a anonymous referee for helpful comments which gave rise to § 5.

REFERENCES

Bicknell, G. V. 1984, ApJ, 286, 68
Cantó, J., & Raga, A. C. 1991, ApJ, 372, 646
Evans, D. S. 1967, in IAU Symp. 30, Determination of Radial Velocities and Their Applications, ed. A. H. Batten & J. F. Heard (London: Academic Press), 57
Josselin, E., Mauron, N., Planesas, P., & Bachiller, R. 2000, A&A, 362, 255
Knapp, G. R., Pourbaix, D., Platais, L., & Jorissen, A. 2003, A&A, 403, 993
Martin, D. C., et al. 2007, Nature, 448, 780
Matthews, L. D., Libert, Y., Gérard, E., Le Bertre, T., & Reid, M. J. 2008, ApJ, 684, 603
Pittard, J. M., Dyson, J. E., Falle, S. A. E. G., & Hartquist, T. W. 2005, MNRAS, 361, 1077
Raga, A. C., Cantó, J., De Colle, F., Esquivel, A., Kajdic, P., Rodríguez-González, A., Velázquez, P. F. 2008, ApJ, 680, L45
Ryde, N., Gustafsson, B., Eriksson, K., & Hinkle, K. H. 2000, ApJ, 545, 945
Turon, C., et al. 1993, Bull. Cent. Donnees Stellaires, 43, 5
Wareing, C. J., Zijlstra, A. A., O'Brien, T. J., & Seibert, M. 2007, ApJ, 670, L125
Winters, J. M., Le Bertre, T., Jeong, K. S., Nyman, L.-Å., & Epchtein, N. 2003, A&A, 409, 715